INL/CON-11-23985
PREPRINT

PHISICS Toolkit: Multi-Reactor Transmutation Analysis Utility – MRTAU

PHYSOR 2012

Andrea Alfonsi
Cristian Rabiti
Aaron S. Epiney
Yaqi Wang
Joshua Cogliati

April 2012

The INL is a
U.S. Department of Energy
National Laboratory
operated by
Battelle Energy Alliance

PHYSOR 2012 – Advances in Reactor Physics – Linking Research, Industry, and Education
Knoxville, Tennessee, USA, April 15-20, 2012, on CD-ROM, American Nuclear Society, LaGrange Park, IL (2012)

PHISICS TOOLKIT: MULTI-REACTOR TRANSMUTATION ANALYSIS UTILITY - MRTAU

Andrea Alfonsi, Cristian Rabiti, Aaron S. Epiney, Yaqi Wang, Joshua Cogliati
Idaho National Laboratory
2525 Fremont Avenue, Idaho Falls, ID 83415, USA
Andrea.Alfonsi@inl.gov

ABSTRACT

The principal idea of this paper is to present the new capabilities available in the PHISICS toolkit, connected with the implementation of the depletion code MRTAU, a generic depletion/ decay/burn-up code developed at the Idaho National Laboratory. It is programmed in a modular structure and modern FORTRAN 95/2003. The code tracks the time evolution of the isotopic concentration of a given material accounting for nuclear reactions happening in presence of neutron flux and also due to natural decay. MRTAU has two different methods to perform the depletion calculation, in order to let the user choose the best on with respect to his needs. Both the methodologies and some significant results are reported in this paper.

Key Words: Bateman, Depletion, Core simulation

1. INTRODUCTION

The main purpose of this paper is to introduce the depletion module **MRTAU** (**M**ulti-**R**eactor **T**ransmutation **A**nalysis **U**tility) [1] implemented in the newly developed Reactor Physics toolkit **PHISICS** (**P**arallel and **H**ighly **I**nnovative **S**imulation for **I**NL **C**ode **S**ystem) [2,3]. This package is intended to provide a modern analysis tool for reactor physics investigation. It is designed with the mindset to maximize accuracy for a given availability of computational resources. This is obtained by implementing several different algorithms and meshing approaches among which the user will be able to choose in order to optimize his computational resources and accuracy needs. The software is completely modular in order to simplify the independent development of modules by different teams and future maintenance. The package is coupled with the thermo-hydraulic code RELAP5-3D [3] and composed by 6 internally developed kernels:

- Neutron transport solver INSTANT (**I**ntelligent **N**odal and **S**emi-structured **T**reatment for **A**dvanced **N**eutron **T**ransport);
- Depletion code MRTAU;
- Time dependent transport driver;
- Cross section manipulation and interpolation module MIXER;
- Criticality Search module;
- Generalized perturbation theory (under development).

MRTAU is a generic depletion/decay/burn-up code developed at the Idaho National Laboratory. It is programmed in a modular structure and modern FORTRAN 95/2003. The code tracks the time evolution of the isotopic concentration of a given material accounting for nuclear reaction happening in presence of neutron flux and also due to natural decay (Bateman equation). Moreover the code can provide as additional output information regarding integral quantities associate to different nuclear reactions like helium production and energy released (pseudo isotopes are used to simulate decay heat). The calculation flow could be controlled in such a way in core and out core periods could be alternated freely.

The new version of the code here presented differs noticeably from the first version (2008) used to simulate sustained multi-recycle of MOX-UE to the point of Cf-252 equilibration (equilibrium cycle) [4]. Initially MRTAU tracked a fixed set of nuclides (27 actinides between U-234 and Cf-252) by hard coded decay-reaction chains and a second order Taylor Series approximation. By further developments in 2009, MRTAU has been equipped with new features such as the Fission Product tracking. This last version has been completely rewritten, new solution algorithms added to the original second order Taylor approximation of the exponential matrix, and no hardcoded libraries are present anymore to give to users a larger degree of freedom to solve their specific problems.

2. MRTAU STRUCTURE AND MAIN FEATURES

As already mentioned, MRTAU has completely been rewritten in a modular approach. It makes extensive use of the FORTRAN derived data types in order to drive effortlessly and optimize the different calculation tasks. This structure makes easier and faster the access to the data and the sharing of them among the different modules. The new input deck of MRTAU is in XML (eXtensible Markup Language) format, but a option to read the old input form has also been preserved to ensure the compatibility with the tools developed by the INL Fuel Cycle Team [12]. The new version of MRTAU, as briefly explained before, has inherited all the features already present in the previous version:

- multi transmutation and partitioning loops;
- possibility for the user to deplete only the actinides or actinides and fission products;
- the calculation can be performed keeping the flux or the thermal power constant (stand-alone mode);
- power history specification;
- separation efficiency specification for each isotope.

The implementation of the code in PHISICS toolkit has been connected with the adding of new important features. The decay/reaction chains are now collected in external libraries, in order to make the code highly customizable. The chain libraries can be modified by the user to track a specific set of isotopes, to add new nuclides or light elements and, in addition, they can be inputted in XML format. In this way the construction of the transmutation matrix is completely user-dependent.

MRTAU has been equipped with a decay heat module and a burn-up/power one. These two new features are pivotal for the coupling with the other elements present in the toolkit.

The most important improvements have been localized on the depletion solvers itself. The Taylor series expansion based algorithm has been optimized through the nonzero matrix multiplication technique and generalized to any arbitrary order. The **C**hebyshev **R**ational **A**pproximation **M**ethod (**CRAM**) for the computation of the exponential matrix has also been added as a new calculation option. The decision to introduce such a new methodology has been driven by the larger stability range [7-8] compared to the classic Taylor method without the need to perform exceptions for short living nuclides like, for example, in ORIGEN [13].As shown in the convergence study paragraph, the CRAM methodology has shown stability in the Xe-135 tracking up to a time step length of ten days out core and 100 days in core.

MRTAU has been parallelized through a “depletion/burning zones” scheme. If the code runs in parallel, the burning zones, specified by input, will be treated in parallel. The following figure shows an example of how the nodes are distributed among the processors (73 nodes, 4 processors).

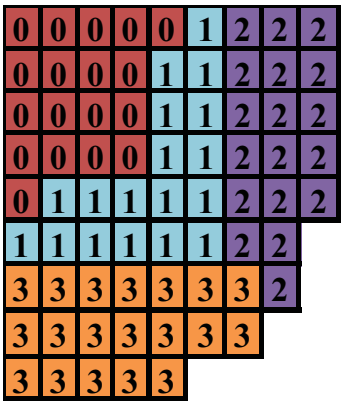

Figure 1 – Parallel distribution of processors

3. THEORY

3.1 Statement of the problem

The main equation solved by MRTAU is the production/destruction equation (Bateman equation).
For each homogeneous region of the reactor core (h) where we assume constant isotopic cross sections, fluxes, and nuclide densities the Bateman equation governing the depletion/burn-up of the material could be written as it follows:

$$\frac{dN_k^h(\mathrm{t})}{dt} = \sum_{i=1}^{actinides} N_i^h(\mathrm{t}) \sum_{g=1}^{G} \varphi^{h,g}(\mathrm{t}) \sigma_{f,i}^{h,g} y_{i\to k}^{g} + \sum_{z=r}^{reactants} N_z^h(\mathrm{t}) \sum_{g=1}^{G} \varphi^{h,g}(\mathrm{t}) \sigma_{c,z}^{h,g} \gamma_{z\to k}^{g}$$
$$+ \sum_{j=n}^{parents} N_j^h(\mathrm{t}) \lambda_j \alpha_{j\to k} - \lambda_k N_k^h(\mathrm{t}) - N_k^h(\mathrm{t}) \sum_{g=1}^{G} \varphi^{h,g}(\mathrm{t}) \sigma_{a,k}^{h,g} \quad (1)$$

Where a pricewise constant approximation has been assumed with respect to the energy dependency (multi-group approximation) and the variables have the following physical meaning:

N_k^h is the atomic density of isotope k, in region h;
$\varphi^{h,g}$ is the neutron flux in energy group g and spatial region h;
$\sigma_{f,i}^{h,g}$ is the microscopic fission cross section for isotope i, in energy group g, and spatial region h;
$\sigma_{c,z}^{h,g}$ is the microscopic capture cross section for isotope z, in energy group g and spatial region h;
$\sigma_{a,k}^{h,g}$ is the microscopic absorption cross section for isotope k, in energy group g and spatial region h;
λ_j is the radioactive decay constant of nuclide j;
λ_k is the radioactive decay constant of nuclide k;
$y_{i\to k}^{g}$ is the probability that a fission of isotope i will produce isotope k for a neutron in energy group g;
$\gamma_{z\to k}^{g}$ is the probability that a neutron capture in nuclide z will produce isotope k for a neutron in energy group g.

What is not shown here is that the neutron flux depend itself from the nuclide density via the definition of the macroscopic cross section. This binding leads to a set of non linear coupled equation. The simplest approach to eliminate this non linearity is to assume that over small time step the fluxes could be assumed constant and compute the effect of the density changes on the flux itself at the end of each time step. This scheme clearly reproduce an operator splitting approach since it decouples, by lagging the coupling term, the transport equation from the Bateman equation.
The operator splitting approach could be formally described by the introduction of a time index (subscript S). Equation (1) for time step Δt_s could be therefore written in the following form:

$$\frac{dN_{k,S}^h}{dt} = \sum_{i=1}^{actinides} N_{i,S}^h \sum_{g=1}^{G} \varphi_{S-1}^{h,g} \sigma_{f,i}^{h,g} y_{i\to k}^g + \sum_{z=r}^{reactants} N_{z,S}^h \sum_{g=1}^{G} \varphi_{S-1}^{h,g} \sigma_{c,z}^{h,g} \gamma_{z\to k}^g + \sum_{j=n}^{parents} N_{j,S}^h \lambda_j \alpha_{j\to k}$$

$$-\lambda_k N_{k,S}^h - N_{k,S}^h \sum_{g=1}^{G} \varphi_{S-1}^{h,g} \sigma_{a,k}^{h,g} \qquad (2)$$

The operator splitting practically is performed as it follows:
- The flux must be found for the desired region using the transport or diffusion equations (performed externally to MRTAU) at time S-1
- This flux is then used in Eq. (2) to determine the isotopic concentrations at time S.
- These new values are used to determine new material properties such as macroscopic cross section to calculate the flux at time S.
- This process is used to march over in time.
  The limit of this approach is of course the assumption that the space-energy-averaged flux can be considered constant over a sufficiently small time interval, Δt. Similarly, it is assumed that a single set of burn-up-dependent neutron cross sections can be used over the same time step. The Bateman equation, as formulated in Eq 2 could be now treated as a linear differential equation.

3.2 Taylor Method

Eq. (2) represents, at each time step, a coupled set of linear, homogeneous, first-order differential equations with constant coefficients. As such, Eq. (2) can be written in matrix notation as

$$\dot{\bar{N}} = -\bar{\bar{A}}\bar{N} \qquad (3)$$

Where:

$\bar{N}$ is a vector of nuclide concentrations;

$\bar{\bar{A}}$ is the transition matrix containing decay/production constants plus absorbtion/fission cross section time the flux.

Given the nuclide concentration at t_{s-1}, $\bar{N}_{s-1}$ and assuming the neutronic flux constant for $t_{s-1} < t < t_s$we can compute the exact nuclide density at t_s. Equation (3) has the solution:

$$\bar{N}_s = \exp\left(-\bar{\bar{A}}_s \Delta t_s\right) \bar{N}_{s-1} \qquad (4)$$

Analogous to a series expansion for the exponential function, the matrix exponential function, $exp\left(\bar{\bar{A}}\Delta t_s\right)$, appearing in Eq.(4), is defined as

$$\exp\left(-\bar{\bar{A}}_s\Delta t_s\right) = \bar{\bar{I}} - \bar{\bar{A}}_s\Delta t_s + \frac{(\bar{\bar{A}}_s\Delta t_s)^2}{2} + \cdots = \sum_{m=0}^{\infty}(-1)^m\frac{(\bar{\bar{A}}_s\Delta t_s)^m}{m!} \cong \sum_{m=0}^{M}(-1)^m\frac{(\bar{\bar{A}}_s\Delta t_s)^m}{m!} \quad (5)$$

with $\bar{\bar{I}}$ being the unit matrix. Equations (4) and (5) constitute the Taylor approximation of the exponential matrix solution of the Bateman equation.

3.3 Solution with the matrix exponential method: CRAM

The Chebyshev rational approximation method (CRAM) is a matrix exponential method that is based on the observation that the eigenvalues of the depletion coefficient matrix $\bar{\bar{A}}$ appear to be close around the negative real axis [8]. This can be exploited by making a Chebyshev rational approximation of the exponential function for the interval (-∞, 0]. The resulting rational function is then decomposed into a pole-residue form to avoid numerical instability. When the denominator and numerator orders are selected equal and even in the Chebyshev approximation, the poles form conjugate pairs and the imaginary parts cancel out leading to a real variable.
Let $\Pi_{k,l}$ represent the collection of all real rational functions $r_{k,l}(x)$ of the form:

$$r_{k,l} = \frac{p_k(x)}{p_l(x)}, \text{where } p_l \text{ is a polynomial of degree l or less} \quad (8)$$

From the approximation theory it is known that there exists an unique $\hat{r}_{k,l} \in \Pi_{k,l}$ that satisfy

$$\sup_{-\infty<x\leq 0}|\hat{r}_{k,l}(-x) - e^x| = \inf_{\hat{r}_{k,l}\in\pi_{k,l}}\left\{\sup_{-\infty<x\leq 0}|\hat{r}_{k,l}(-x) - e^x|\right\}, k \leq l \quad (9)$$

To find $\hat{r}_{k,l}$ for a given k and l is not easy, but it can be done via the Remez algorithm [10]. It is extremely useful, for the application of the method, to consider a formulation with l=k (CPU time). It's been shown that $\hat{r}_{k,k}$ converges at the rate 9.3^{-k} to the exact exponential matrix representation. The final form of the approximating expression is reported below:

$$\hat{r}_{k,k}(z) = k_d + \sum_{i=1}^{k}\frac{re_i}{z - po_i} \quad (10)$$

Where k_d is the limit of the function at infinity and the scalars re_i are the residues at the poles po_i.
The fact that the poles $\{po_1 \ldots po_k\}$ of the rational function $\hat{r}_{k,k}$ are distinct, allows computing it as a partial fraction expansion. As expected in an optimization problem the values of re_i and po_i depend on the global order of expansion k. As explained above, the poles of $\hat{r}_{k,k}$ are conjugate pairs, therefore for a real-valued variable$x \in \mathbb{R}$, the computational cost can be helve:

$$\hat{r}_{k,k}(z) = k_d + 2Re\left(\sum_{i=1}^{k/2}\frac{re_i}{z - po_i}\right), k\ even \quad (11)$$

$$\hat{r}_{k,k}(z) = k_d + \left\{2Re\left(\sum_{i=1}^{k/2}\frac{re_i}{z - po_i}\right) + \frac{re_k}{z - po_k}\right\}, k\ odd \quad (12)$$

where *k/2* is an integer division.
When this approximation is applied to the matrix exponential representing the Bateman equation (3), it becomes:

$$\overline{N}_{t+\Delta t} = k_d \overline{N_t} - 2Re\left(\sum_{i=1}^{k/2} \frac{re_i}{\left(\bar{\bar{A}}\Delta t + po_i \bar{\bar{I}}\right)}\right)\overline{N_t}, k\ even \tag{13}$$

$$\overline{N}_{t+\Delta t} = k_d \overline{N_t} - \left\{2Re\left(\sum_{i=1}^{k/2} \frac{re_i}{\left(\bar{\bar{A}}\Delta t + po_i \bar{\bar{I}}\right)}\right) + \frac{re_k}{\left(\bar{\bar{A}}\Delta t + po_k \bar{\bar{I}}\right)}\right\}\overline{N_t}, k\ odd \tag{14}$$

The matrix inversions can be calculated efficiently thank to the sparse structure of the matrix $\bar{\bar{A}}$ Using the LAPACK package [14].
It is easily understandable that it is not convenient to compute the CRAM of an odd degree, since the matrix inversions to be performed in this case are the same of those must be computed in a higher, by one, order approximation.

3.3.1 Remez algorithm

The Chebyshev coefficients (pole-residue form) are tabulated in an internal MRTAU library up to the 30th order. This tabulation has been obtained using an internal subroutine of the PHISICS package that uses the Remez Algorithm and perform the partial fraction decomposition. In case the required order is higher the code will automatically use this tool to collect the missed coefficients.
This module is based on the mini-max Remez algorithm [10]. The mini-max approximation seeks the polynomial of degree *n* that approximates the given function (in our case e^x) in the given interval such that the absolute maximum error (the difference between the function and the polynomial) is minimized. As explained before through the equation (9), Chebyshev proved that such polynomial exists and that it is unique and gave the criteria to asses if a polynomial is a mini-max polynomial. Although the algorithm is applicable for a generic function *F(x)*, here it will be described for the particular case of $F(x) = e^x$. Assuming that the given interval is [*a, b*], Chebyshev's criteria states that if $P_n(X)$ is the mini-max polynomial of degree *n* then there must be at least (*n*+2) points in this interval at which the error function attains the absolute maximum value with alternating sign and by the following equations:

$$e^{x_i} - P_n(x_i) = (-1)^i E \tag{15}$$

$$e^{x_i} - [c_0 + c_1(x_i - a) + c_2(x_i - a)^2 + \cdots + c_n(x_i - a)^n] = (-1)^i E \tag{16}$$

$$c_0 + c_1 h_i + \cdots + c_n h_i^n + (-1)^i E = e^{x_i} \tag{17}$$

$$i = 0,1,2, \ldots, n+1$$

Equation (17) is a system of (*n* + 2) linear equations in the (*n* + 2) unknowns $\{c_0, c_1, \ldots, c_n, E\}$. These equations are proved to be independent hence they can be solved using any method from linear algebra to get the values of the coefficients as well as the error at the given (*n* + 2) points. After the first step the coefficients are computed such that the error function at the given (*n* + 2) points is equal in magnitude and alternating in sign. The magnitude of this error is not the absolute maximum in the given interval [*a, b*] and the mini-max criterion is not still satisfied. It is needed to move to a new set of points. The second step of Remez algorithm, called "exchange step", seeks a new set of (*n* + 2) points that approach the (*n* + 2) points of the mini-max condition. In this exchange step, all the points of the current set of (*n* + 2) points are exchanged to get new set points.

It can be noted that the error alternates in sign at the (n + 2) points of the first step therefore the error function has (n + 1) roots, one root in each of the intervals (Fig.1): [x_0, x_1], [x_1, x_2], . . . , [x_n, x_n+1]. These roots can be computed using any numerical root finding algorithm. Denoting these roots by $z_0, z_1, \ldots, z_n$, the interval [a, b] is divided into the (n + 2) intervals: [a, z_0], [z_0, z_1], [z_1, z_2], ..., [z_n−1, z_n], [z_n, b]. In each of these intervals, it is calculated the point at which the error attains its maximum or minimum value (x_0*, x_1*, ..., x_{n+1}*). The last step can be carried out numerically by computing the root of the derivative of the error function if such root exists, otherwise the error function at the endpoints of the interval is computed and it is picked the one that gives larger absolute value. Let define k such that

$$k = \max_i |e^{x_i^*} - P_n(x_i^*)| \tag{18}$$

After the exchanging step, this new set of (n + 2) points is used in the first step of the following iteration. The two steps are repeated a number of times until the difference between the old (n + 2) points and the new (n + 2) ones lie below a given threshold.

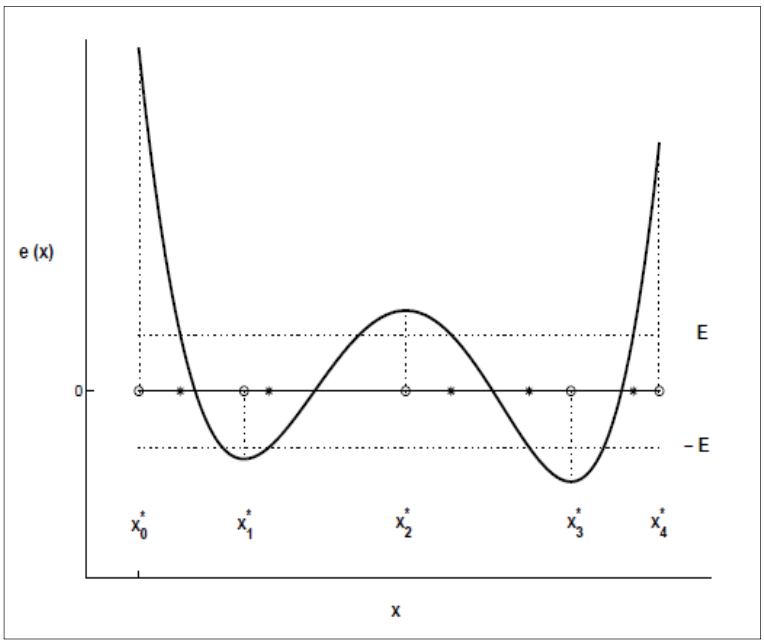

Figure 2 – Remez algorithm second step.

4. APPLICATIONS AND RESULTS

In this section some results are shown in order to attest the capabilities of the code itself and its implementation inside the PHISICS toolkit environment. The first subsection refers to the convergence analysis performed to verify the two matrix exponential methods used by MRTAU. The second subsection presents the results of the benchmark [11].
The first test is a self comparison of the two methodologies implemented while in the second we compare with a literature benchmark the CRAM implementation. It is outside of the scope of this paper to provide a validation of the libraries.

4.1 Convergence analysis

As already mention the in the first test the convergence of the two methodologies has been verified in a comparative test. The main test case specifications are collected in the table below.

Table I – Convergence test case specifications

Specifications				Notes
Cycle Length (days)	300.0			
Power history steps	3			100 days each
Power history (% of nominal power)	0.0 %	100.0 %	0.0 %	
Actinides – Fission products tracked	29	182		
Fuel	MOX 10% enrichment			

This study has been performed through more than 70 calculations, acting on the order of the methods and the number of time steps (as shown in the tables II and III).

Table II – CRAM calculation run

Chebyshev Rational Approximation Method							
TS number	Approximation Order						
3	IV	VI	VIII	X	XII	XIV	
30	IV	VI	VIII	X	XII	XIV	
300	IV	VI	VIII	X	XII	XIV	
3000	II	IV	VI	VIII	X	XII	XIV
30000	XIV	→ Reference					

Table III – Taylor calculation run

Taylor Series Approximation Method									
TS number	Approximation Order								
30	II	III	IV	V	VI	VII	VIII	IX	X
300	II	III	IV	V	VI	VII	VIII	IX	X
3000	II	III	IV	V	VI	VII	VIII	IX	X
30000	II	III	IV	V	VI	VII	VIII	IX	X
300000	II	III	IV	V	VI	VII	VIII	IX	X

Three isotopes have chosen as representative of three isotope groups based on half life:

- I Group - Actinides: Isotope representative Pu-239;
- II Group - Fission products (half life > 0.5 years): Isotope representative Kr-85;
- III Group - Fission products (half life < 0.5 years): Isotope representative Xe-135.

The reference is given by the 14th order CRAM approximation with a time step length of 864 seconds (30,000 time steps).
The comparative test has been performed computing the relative errors for each representative isotope, order and time step number.
The two points in time here reported are those at 200 (100 cooling and 100 in core) and 300 days (post-burning cooling). As expected, the III group is the stiffest one and for that reason only its relative errors are reported (Table IV and V).

Table IV – Taylor Series relative error III group

Taylor Series – Relative error (%)									
Post-burning cooling – III Group									
Order / TS number	II	III	IV	V	VI	VII	VIII	IX	X
30	100.000	100.000	100.000	100.000	100.000	100.000	100.000	100.000	100.000
300	100.000	100.000	100.000	100.000	100.000	100.000	100.000	100.000	100.000
3000	100.000	73.980	73.190	73.190	73.190	73.190	73.190	73.190	73.190
30000	1.023	0.508	0.507	0.507	0.507	0.507	0.507	0.507	0.507
300000	0.177	0.172	0.170	0.169	0.169	0.169	0.169	0.169	0.169
Initial cooling + burning – III Group									
30	100.000	100.000	100.000	100.000	100.000	100.000	100.000	100.000	100.000
300	100.000	0.000	0.000	0.000	0.000	0.000	0.000	0.000	0.000
3000	0.000	0.000	0.000	0.000	0.000	0.000	0.000	0.000	0.000
30000	0.000	0.000	0.000	0.000	0.000	0.000	0.000	0.000	0.000
300000	0.000	0.000	0.000	0.000	0.000	0.000	0.000	0.000	0.000

Table V – CRAM relative error III group

CRAM – Relative error (%)							
Post-burning cooling – III Group							
Order / TS number	II	IV	VI	VIII	X	XII	XIV
3	100.000	100.000	100.000	100.000	100.000	100.000	100.000
30	100.000	100.000	100.000	100.000	10.240	0.120	0.001
300	100.000	100.000	0.157	0.002	0.001	0.000	0.000
3000	100.000	1.256	0.657	0.001	0.000	0.000	0.000
Initial cooling + burning – III Group							
3	100.000	15.880	0.201	0.002	0.000	0.000	0.000
30	100.000	1.707	0.019	0.000	0.000	0.000	0.000
300	100.000	1.647	0.006	0.000	0.000	0.000	0.000
3000	100.000	0.006	0.001	0.000	0.000	0.000	0.000

The following graphs show the order and the time step size for which the condition (relative error) < 0.3% was satisfied. In the graphs, the region above the lines is the one with the error under the above specified value. It could be depicted, for example, that the after irradiation situation is the most difficult to capture in fact the curves rise earlier (thus it is required an higher degree of accuracy for a given time-step size) Another consideration that arises from the analysis of the results is that CRAM below the 4th order has problem but overall it can effort large time step, while Taylor has a low sensibility to the order and require smaller time step. The poor performance of CRAM at low order is a well know phenomena [5] while the low impact of the order on the Taylor method is probably due to numerical round off that could be probably improved.

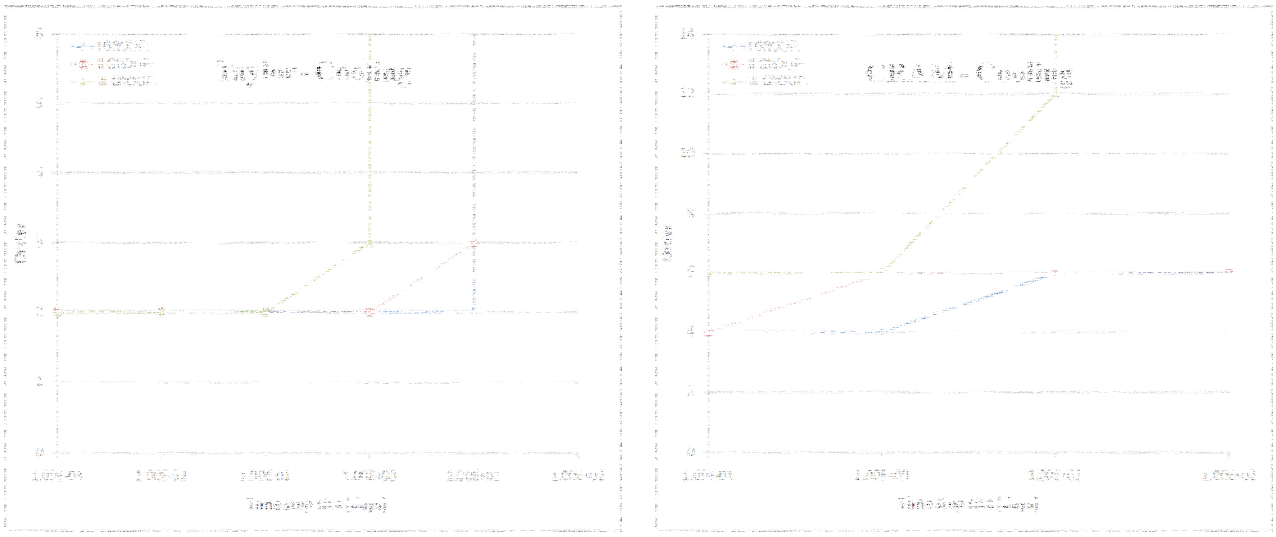

Figure 3 - Decay accuracy curves

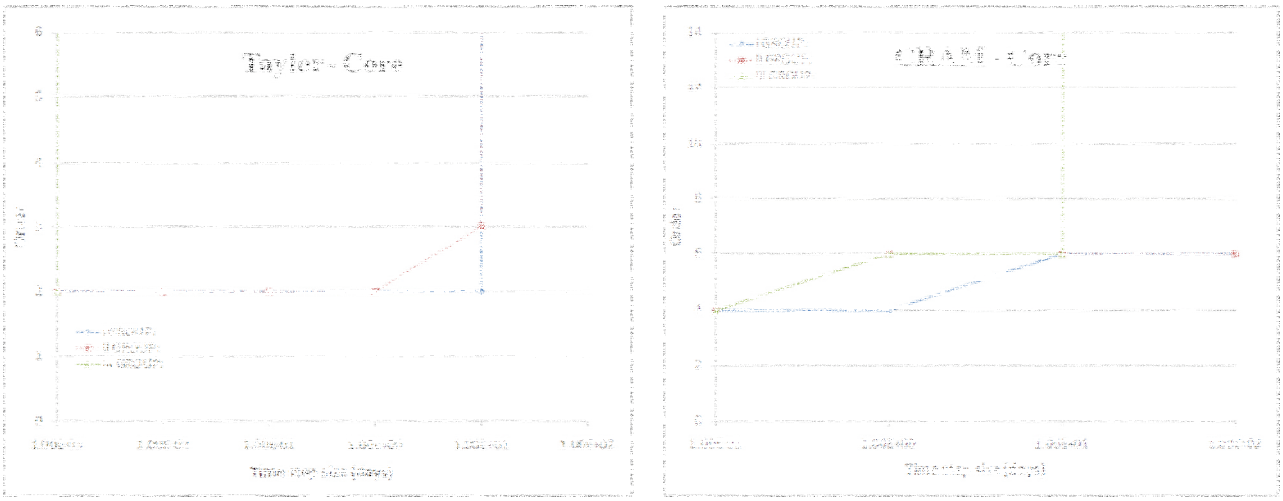

Figure 4 - Burning accuracy curves

The following table gives a good indication on the computational time of both methodologies[1]. The Chebyshev rational approximation method is not penalized in term of order-to-order comparison with Taylor, even if it requires several inversion of the transmutation matrix. This is due by the much stronger optimization performed on this methodology.

Table VI – Computational Time (single processor)

Computational time (sec/iteration)											
Method	**Approximation Order**										
	II	**III**	**IV**	**V**	**VI**	**VII**	**VIII**	**IX**	**X**	**XII**	**XIV**
Taylor	0.0155	0.0177	0.0198	0.0225	0.0250	0.0275	0.0302	0.0327	0.0352	/	/
CRAM	0.0069	/	0.0079	/	0.0087	/	0.0095	/	0.0103	0.0111	0.0119

4.2 Two-dimensional PWR model, two load cycle model

4.2.1 Specifications

This benchmark, proposed by K. Koebke, R. Wagner at all in 1985 [11], has been designed to provide a test for the capabilities of coarse mesh methods for PWR fuel management calculations. It is set up to allow the use of computer codes which model either a quarter of a core or a reactor octant. The 2D geometry consists of 5 assembly types, characterized by different cross sections and compositions (presence or absence of burnable poison - BP). The benchmark is a two groups and two depletion cycles problem. The reactor is maintained critical at all times by adjusting the amount (ppm) of soluble boron (SB). The Xenon in the benchmark is treated as in equilibrium while we solve the transient equation (Bateman). The scattering matrix is given as a macro cross section attributed to the structural material STRM. The cycle length is defined by requiring the critical boron concentration to become equal to zero.
Since a refueling pattern module is not present in the PHISICS package so far, it has been decided to run the first cycle only and not to model the insertion of the control rods at the begin of the cycle. The problem has been solved considering 3 different models, in order to certify the convergence trend:

I. 5 depletion zones, corresponding to the different assembly types;
II. 56 depletion zones, one for assembly;
III. 504 depletion zones, 9 nodes for assembly.

The square assemblies have a side 23.0 cm long and the global dimension of the core is approximately 195.5 x 195.5 cm.
The initial nuclide densities and the assembly/core geometry are summarized in the tables below, where the initials “C.S.” mean the densities are computed through the criticality search module and the assembly type 6 is the reflector (modeled by macro cross sections).

[1] PC: Intel Core 2 Duo, CPU E8400 3.00 GHz, 3.25 GB of RAM.

Table VII – Initial densities

Initial Densities (Atoms/(barn*cm))					
	Type 1	**Type 2**	**Type 3**	**Type 4**	**Type 5**
U235	1.40E-4	1.60E-4	1.60E-4	2.20E-4	2.20E-4
U236	0.00E+0	0.00E+0	0.00E+0	0.00E+0	0.00E+0
U238	6.31E-03	6.29E-03	6.29E-03	6.23E-03	6.23E-03
PU239	0.00E+0	0.00E+0	0.00E+0	0.00E+0	0.00E+0
PU240	0.00E+0	0.00E+0	0.00E+0	0.00E+0	0.00E+0
PU241	0.00E+0	0.00E+0	0.00E+0	0.00E+0	0.00E+0
PU242	0.00E+0	0.00E+0	0.00E+0	0.00E+0	0.00E+0
XE135	0.00E+0	0.00E+0	0.00E+0	0.00E+0	0.00E+0
BP	0.00E+0	0.00E+0	8.00E-06	0.00E+0	8.00E-06
FP	0.00E+0	0.00E+0	0.00E+0	0.00E+0	0.00E+0
SB	C.S.	C.S.	C.S.	C.S.	C.S.

Table VIII – Quarter core geometry

1	3	1	3	1	3	2	5	6
3	1	3	1	3	1	3	4	6
1	3	1	3	1	3	1	5	6
3	1	3	1	3	1	5	4	6
1	3	1	3	1	3	4	6	6
3	1	3	1	3	2	5	6	
2	3	1	5	4	5	6	6	
5	4	3	4	6	6	6		
6	6	6	6	6				

4.2.2 Results

The results of the first model (5 depletion zones) will not be shown in this paper, excepting the end of cycle time, since the relative errors are too large.
The following tables and graphs summarize the main results obtained by the three different models, focusing the attention on the end of cycle time, critical boron concentration evolution and the relative errors for the final nuclide densities per Fuel Batch.

Table IX – End of cycle time

End of cycle (days)				
Depletion Regions / Time Steps	**5**	**56**	**504**	**Benchmark reference**
45	410.11	399.44	393.11	381.49
100	409.10	398.43	392.09	

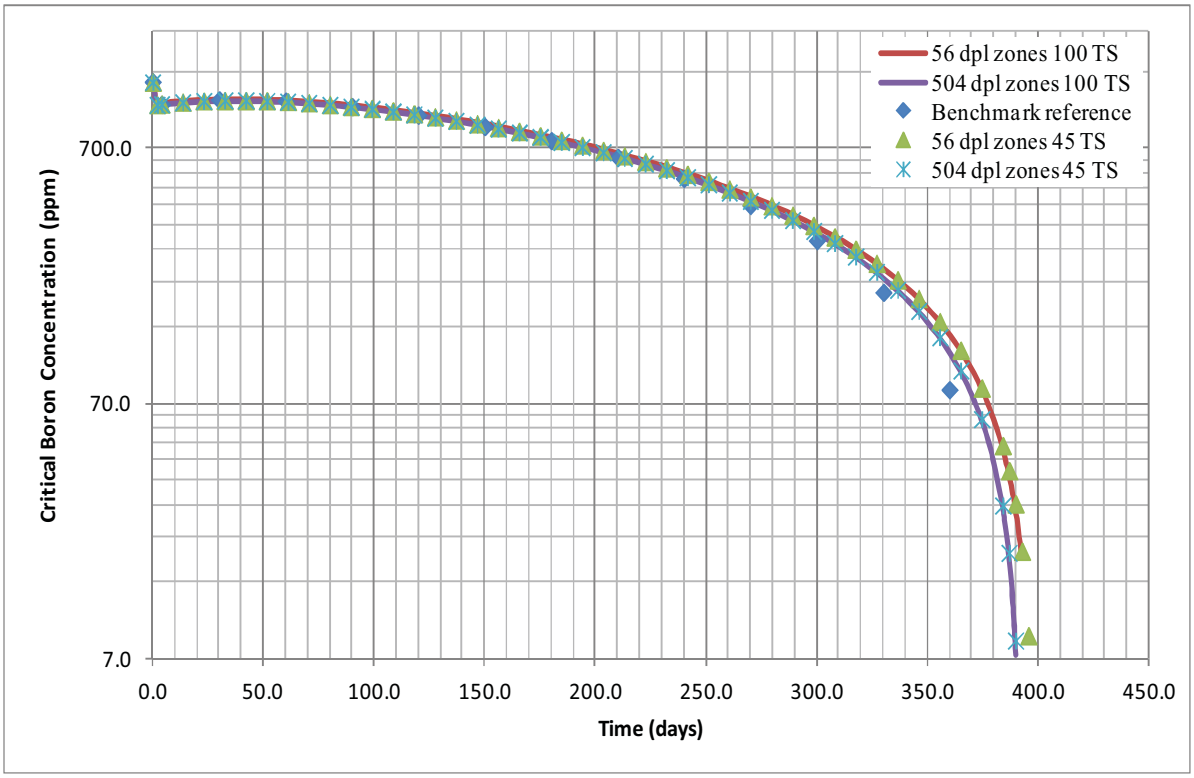

Figure 5 – Critical boron concentration evolution

The two tables below show the relative errors for the nuclide densities at the end of cycle and at the benchmark reference value for that.

Table X – Relative errors for nuclide densities for each fuel batch at EOC

Time (days)	392.09		**Regions**	504	
Nuclide	**A type 1**	**A type 2**	**A type 3**	**A type 4**	**A type 5**
U235	-2.33%	-2.07%	-2.31%	-1.28%	-1.33%
U236	1.77%	2.14%	1.95%	2.58%	2.55%
U238	-0.04%	-0.03%	-0.04%	-0.02%	-0.03%
PU239	0.72%	0.99%	0.69%	1.72%	1.60%
PU240	2.37%	2.89%	2.43%	3.69%	3.55%
PU241	4.52%	5.33%	4.84%	5.89%	5.87%
PU242	8.29%	9.22%	8.90%	8.87%	9.18%
XE135	-0.20%	-0.30%	-0.34%	-0.19%	-0.23%
FP	-4.25%	-3.12%	-3.93%	-1.35%	-1.62%
BP	/	/	-6.42%	/	-3.76%

Table XI – Relative errors for nuclide densities for each fuel batch at benchmark reference EOC

Time (days)	381.00		Regions	504	
Nuclide	**A type 1**	**A type 2**	**A type 3**	**A type 4**	**A type 5**
U235	0.20%	0.08%	0.09%	0.04%	0.04%
U236	-0.12%	-0.07%	-0.06%	-0.03%	-0.06%
U238	0.00%	0.00%	0.00%	0.00%	0.00%
PU239	0.13%	0.10%	0.06%	0.21%	0.14%
PU240	0.00%	0.00%	0.00%	-0.14%	-0.16%
PU241	-0.19%	-0.18%	-0.10%	-0.82%	-0.67%
PU242	-0.55%	-0.46%	-0.28%	-0.90%	-0.80%
XE135	0.11%	0.00%	0.04%	0.03%	-0.02%
FP	-0.20%	-0.10%	-0.08%	-0.07%	-0.05%
BP	/	/	0.25%	/	-0.14%

5. CONCLUSIONS

The main purpose of this paper was to present the new capabilities in the PHISICS toolkit, connected with the depletion module MRTAU. The convergence test has demonstrated and verified the two methodologies converge to the same values and the different stability requirements. The CRAM is highly dependent on the order of the approximation but weakly from the time step size (above the 8^{th} with 100 days time step in core the Xe-135 is accurate); the Taylor series method is dependent on the length of the time step instead. Thus, it is advisable to choose the Chebyshev rational approximation in calculations characterized by the possibility of using very long time steps. The benchmark results had the main purpose to testify the capabilities of the entire package. Since the end of cycle is about 10 days off, the final densities are affected by large relative errors. These errors are very small if we would instead compare the densities at the 381 days where the calculation in the reported results ends. The depletion capability of PHISICS has been tested and results are congruent therefore this could be a new highly flexible tool in the hands of nuclear engineers.

ACKNOWLEDGMENTS

This work is supported by the U.S. Department of Energy, under DOE Idaho Operations Office Contract DE-AC07-05ID14517. Accordingly, the U.S. Government retains a nonexclusive, royalty-free license to publish or reproduce the published form of this contribution, or allow others to do so, for U.S. Government purposes.

REFERENCES

1. S. Bays, S. Piet, M. Pope, G. Youinou, A. Dumontier, D. Hawn, "Transmutation Dynamics: Impacts of Multi-Recycling on Fuel Cycle Performances," INL/EXT-09-16857 (2009).
2. C. Rabiti, Y. Wang, G. Palmiotti, H. Hiruta, J. Cogliati, A. Alfonsi, A. Epiney, T. Grimmet "PHISICS: New Features and Advancements," *Proceedings of American Nuclear Society 2011 Annual Winter Meeting*, Washington, D. C., USA, October 30-November 3 (2011).
3. C. Rabiti, Y. Wang, G. Palmiotti, H. Hiruta, J. Cogliati, A. Alfonsi "PHISICS: a New Reactor Physics Analysis Toolkit," Proceedings American Nuclear Society 2011 Annual Meeting, Hollywood, Florida, USA, June 27-30 (2011).
4. The RELAP5 Development Team, "RELAP5/MOD3 Code Manual," NUREG/CR-5535, INEL-95/0174, Idaho National Engineering Laboratory, August 1995, Vols. 1 and 2.
5. C.Moler, C.Van Loan, "*Nineteen Dubious Ways to Compute the Exponential of a Matrix, Twenty-Five Years Later*", Society for Industrial and Applied Mathematics, 2003.
6. H. Bateman, *"Solution of a system of differential equations occurring in the theory of radio-active transformations"*, Math. Proc. Cambridge 15, pp. 423-427, 1910.
7. A.E. Isotalo, P.A. Aarnio, *"Comparison of depletion algorithms for large systems of nuclides"*, Aalto University, Department of applied physics, 2010.
8. M. Pusa, J. Leppanen, *"Computing the Matrix exponential in Burn-up Calculations"*, VTT Technical Research Centre of Finland, 2009.
9. J. Cetnar, *"General solution of Bateman equations for nuclear transmutations"*, AGH-University of Science and Technology – Faculty of Physics and Applied Computer Sciences, Poland, 2006.
10. S. A. Tawfik, *"Mini-max Approximation and Remez Algorithm",* 2005.
11. K.Koebke, M. R. Wagner et al*., "Two-dimensional PWR Model, Two Load Cycles"*, American Nuclear Society, January 1984.
12. S. J. Piet, N. R. Soelberg, et al., *"The FIT Model – Fuel Cycle Integration and Tradeoffs",* INL/EXT-10-20190, June 2011.
13. L.C. Gauld, O.W. Herman, R.M. Westfall, *"Origen-S: Scale system module to calculate fuel depletion, actinide transmutation, fission product buildup and decay, and associated radiation source terms"*, Oak Ridge National Laboratory, 2009.
14. "LAPACK – Linear Algebra PACKage", http://www.netlib.org/lapack, 2011.